JOURNAL OF THEORETICAL AND APPLIED MECHANICS
50, 2, pp. 563-575, Warsaw 2012
50th Anniversary of JTAM

SIMILARITY SOLUTIONS FOR A CYLINDRICAL SHOCK WAVE IN A ROTATIONAL AXISYMMETRIC GAS FLOW

J.P. Vishwakarama
Prerana Pathak

D.D.U. Gorakhpur University, Department of Mathematics and Statistics, Gorakhpur, India
e-mail: jpv_univgkp@yahoo.com; preranapathak18@gmail.com

Similarity solutions are obtained for an adiabatic flow behind a cylindrical shock wave propagating in a rotational axisymmetric flow of a perfect gas, in which initial velocity and density are functions of the distance from the axis of symmetry. The initial medium is considered to have a variable azimuthal velocity component in addition to the variable axial velocity. Initial velocities and density are assumed to obey power laws. Distributions of the fluid velocities, density, pressure and vorticity components are obtained in the flow-field behind the shock front. Effects of variable initial velocities and density and the variation of the shock-Mach number are investigated.

Key words: shock wave, axisymmetric flow, rotating medium, adiabatic flow

1. Introduction

The formulation of self-similar problems and examples describing adiabatic motion of non-rotating gas models of stars, are considered by Sedov (1959), Zel'dovich and Raizer (1967), Lee and Chen (1968) and Summers (1975). Rotation of stars significantly affects the process taking place in their outer layers. Therefore, question connected with the explosions in rotating gas atmospheres are of definite astrophysical interest. Chaturani (1970) studied the propagation of cylindrical shock waves through a gas having solid body rotation, and obtained the solutions by a similarity method adopted by Sakurai (1956). Nath *et al.* (1991) obtained the similarity solutions for the flow behind spherical shock waves propagating in a non-uniform rotating interplanetary atmosphere with increasing energy. Recently, Vishwakarma and Vishwakarma (2007) and Vishwakarma *et al.* (2007) obtained the similarity solution for magnetogasdynamic

cylindrical shock waves propagating in a rotating medium which is a perfect gas with variable density or a non-ideal gas with constant density. In all of the works mentioned above, the ambient medium is supposed to have only one component of velocity, that is the azimuthal component.

In the present work, we obtained the self-similar solutions for the flow behind a cylindrical shock wave propagating in a rotational axisymmetric perfect gas flow which has a variable azimuthal fluid velocity together with a variable axial fluid velocity (Levin and Skopina, 2004). The shock-Mach number is not infinite, but has a finite value. The fluid velocities and the density in the ambient medium are assumed to obey power laws. It is expected that such fluid velocity and density may occur in the atmosphere of rotating planets and stars.

Distribution of the velocities, density, pressure and vorticity components in the flow-field behind the shock are obtained. The effects of change in the index of variation of initial velocity of the medium, the index of variation of the initial density and the variation of the shock-Mack number are investigated.

2. Basic equations and boundary conditions

The fundamental equations governing an unsteady adiabatic axisymmetric rotational flow of a perfect gas, in which heat conduction and viscous stress are negligible, are (Levin and Skopina, 2004)

$$\begin{aligned}
&\frac{\partial\rho}{\partial t}+u\frac{\partial\rho}{\partial r}+\rho\frac{\partial u}{\partial r}+\frac{\rho u}{r}=0 && \frac{\partial u}{\partial t}+u\frac{\partial u}{\partial r}+\frac{1}{\rho}\frac{\partial p}{\partial r}-\frac{v^2}{r}=0\\
&\frac{\partial v}{\partial t}+u\frac{\partial v}{\partial r}+\frac{uv}{r}=0 && \frac{\partial w}{\partial t}+u\frac{\partial w}{\partial r}=0\\
&\frac{\partial}{\partial t}\Big(\frac{p}{\rho^\gamma}\Big)+u\frac{\partial}{\partial r}\Big(\frac{p}{\rho^\gamma}\Big)=0
\end{aligned} \tag{2.1}$$

where ρ, p are density and pressure; u, v and w are the radial, azimuthal and axial components of the fluid velocity $\overline{q}$ in the cylindrical coordinates (r,θ,z); t is time and γ is the ratio of the specific heats of the gas. Also

$$v=rK \tag{2.2}$$

where K is the angular velocity of the medium at the radial distance r from the axis of symmetry. In this case, the vorticity vector $\boldsymbol{\zeta}=1/2$ Curl $\boldsymbol{q}$ has the components

$$\zeta_r = 0 \qquad \zeta_\theta = -\frac{1}{2}\frac{\partial w}{\partial r} \qquad \zeta_z = \frac{1}{2r}\frac{\partial rv}{\partial r} \tag{2.3}$$

The above system of equations should be supplemented with an equation of state. Perfect gas behaviour of the medium is assumed, so that

$$p = \Gamma\rho T \qquad U_m = C_v T = \frac{p}{\rho(\gamma - 1)} \tag{2.4}$$

where Γ is the gas constant, T – temperature, U_m – internal energy per unit mass of the gas and $C_v = \Gamma/(\gamma - 1)$ is the specific heat at constant volume.

We assume that a cylindrical shock wave is propagating outwards from the axis of symmetry in a perfect gas with variable density, which has zero radial velocity, variable azimuthal velocity and variable axial velocity. Jump conductions across the moving shock are

$$\begin{aligned} &u_1 = (1-\beta)\dot{R} && v_1 = v_0 && w_1 = w_0 \\ &\rho_1 = \frac{\rho_0}{\beta} && p_1 = p_0 + (1-\beta)\rho_0\dot{R}^2 \end{aligned} \tag{2.5}$$

where $\dot{R} = dR/dt$ denotes the shock velocity, R is the shock radius and subscripts 0 and 1 refer to the values just ahead and just behind the shock, respectively. The quantity β is given by the equation

$$\beta = \frac{\gamma - 1 + 2M^{-2}}{\gamma + 1} \tag{2.6}$$

where M, the shock-Mach number referred to the speed of sound in the perfect gas $\sqrt{\gamma p_0/\rho_0}$, is given by

$$M = \frac{\dot{R}}{\sqrt{\frac{\gamma p_0}{\rho_0}}} \tag{2.7}$$

Following Levin and Skopina (2004), we obtain the jump conditions for the components of the vorticity vector across the shock as

$$\zeta_{\theta_1} = \frac{1}{\beta}\zeta_{\theta_0} \qquad \zeta_{z_1} = \frac{1}{\beta}\zeta_{z_0} \tag{2.8}$$

Ahead of the shock, the velocity components and the density are assumed to vary as

$$\begin{aligned} &u_0 = 0 && v_0 = BR^b \\ &w_0 = AR^a && \rho_0 = DR^d \end{aligned} \tag{2.9}$$

where a, b, d, A, B, D are constants.

Therefore, from (2.1)

$$p_0 = \frac{B^2 D}{2b+d} R^{2b+d} \qquad 2b+d>0 \tag{2.10}$$

Ahead of the shock, the components of the vorticity vector, therefore, vary as

$$\zeta_{r_0} = 0 \qquad \zeta_{\theta_0} = -\frac{aAR^{a-1}}{2} \qquad \zeta_{z_0} = \frac{(b+1)BR^{b-1}}{2} \tag{2.11}$$

From equations (2.2) and (2.9), we find that the initial angular velocity varies as

$$K_0 = BR^{b-1} \tag{2.12}$$

It decreases as the distance from the axis increases, if $b-1<0$.

The total energy E of the flow-field behind the shock is not constant, but assumed to be time dependent and varying as (Rogers, 1958; Freeman, 1968; Director and Dabora, 1977)

$$E = E_0 t^s \qquad s \geqslant 0 \tag{2.13}$$

where E_0 and s are constants. The positive values of s correspond to the class in which the total energy increases with time. This increase can be achieved by the pressure exerted on the fluid by an expanding surface (a contact surface or a piston). This surface may be, physically, the surface of a stellar corona or condensed explosives or a diaphragm containing a very high-pressure driver gas. By sudden expansion of the stellar corona or the detonation products or the driver gas into the ambient gas, a shock wave is produced in the ambient gas. The shocked gas is separated from this expanding surface, which is a contact discontinuity. This contact surface acts as a 'piston' for the shock wave. Thus the flow is headed by a shock front and has an expanding surface as the inner boundary.

3. Self-similarity transformations

We introduce the following similarity transformations to reduce the equations of motion into ordinary differential equations (Vishwakarma and Yadav, 2003)

$$\begin{aligned} &u = \dot{R}U(\eta) \qquad v = \dot{R}V(\eta) \qquad w = \dot{R}W(\eta) \\ &\rho = \rho_0 g(\eta) \qquad p = \rho_0 \dot{R}^2 P(\eta) \end{aligned} \tag{3.1}$$

where U, V, W, g and P are functions of the non-dimensional variable η only, and

$$\eta = \frac{r}{R} \tag{3.2}$$

The total energy of the perfect gas behind the shock is given by

$$E = 2\pi \int_{R_p}^{R} \Big[\frac{1}{2}\rho(u^2 + v^2 + w^2) + \frac{p}{\gamma - 1}\Big] r \, dr = E_0 t^s \tag{3.3}$$

where R_p is the radius of the inner expanding surface. Applying similarity transformations (3.1) to (3.2) in relation (3.3), we find that the motion of the shock front is given by the equation

$$\frac{E_0 t^s}{2\pi J} = R^2 \dot{R}^2 \rho_0 \tag{3.4}$$

where

$$J = \int_{\eta_p}^{1} \Big[\frac{1}{2} g(U^2 + V^2 + W^2) + \frac{P}{\gamma - 1}\Big] \eta \, d\eta \tag{3.5}$$

η_p being the value of η at the inner expanding surface.

For similarity solutions, the shock-Mach number M (which occurs in shock conditions (3.11)) must be a constant parameter. Therefore, from (2.7)

$$\dot{R} = QR^b \tag{3.6}$$

where Q is a constant. From equation (3.6), on integration

$$R = [(1 - b)Q]^{\frac{1}{1-b}} t^{\frac{1}{1-b}} \tag{3.7}$$

Also, from equation (3.4), we get

$$R = \Big(\frac{E_0}{2\pi J}\Big)^{\frac{1}{2b+d+2}} \Big(\frac{1}{Q^2 d}\Big)^{\frac{1}{2b+d+2}} t^{\frac{s}{2b+d+2}} \tag{3.8}$$

Comparing equations (3.7) and (3.8), we get

$$2b + d = s(1 - b) - 2 \tag{3.9}$$

From equations (2.9), (2.10), (3.6) and (2.7), we obtain

$$\frac{B}{Q} = \frac{1}{M}\sqrt{\frac{2b + d}{\gamma}} \tag{3.10}$$

Then, shock conditions (2.5) are transformed into

$$\begin{aligned} U(1) &= 1-\beta & V(1) &= \frac{1}{M}\sqrt{\frac{2b+d}{\gamma}} & W(1) &= \frac{A}{Q} \\ g(1) &= \frac{1}{\beta} & P(1) &= \tfrac{1}{\gamma M^2}+1-\beta \end{aligned} \tag{3.11}$$

where $a = b$.

The condition to be satisfied at the inner boundary surface is that the velocity of the fluid is equal to the velocity of inner boundary itself. This kinematic condition from (3.1) and (3.2) can be written as

$$U(\eta_p) = \eta_p \tag{3.12}$$

Using transformations (3.1), equations of motion (2.1) take the form

$$\begin{aligned} &-(\eta-U)g' + gU' + g\Big(d+\frac{U}{\eta}\Big) = 0 \\ &-(\eta-U)U' + bU + \frac{P'}{g} - \frac{V^2}{\eta} = 0 \\ &-(\eta-U)V' + V\Big(b+\frac{U}{\eta}\Big) = 0 \\ &-(\eta-U)W' + bW = 0 \\ &-(\eta-U)P' + \frac{(\eta-U)P\gamma g'}{g} + Pd + 2bP - P\gamma d = 0 \end{aligned} \tag{3.13}$$

where the prime denotes differentiation with respect to η. From equations (3.13), we have

$$\begin{aligned} U' &= \frac{1}{\gamma P-(\eta-U)}\Big[\frac{v^2 g(\eta-U)}{\eta} - \frac{P\gamma U}{\eta} - b(\eta-U)Ug - Pd - 2bP\Big] \\ V' &= \frac{V}{\eta-U}\Big(b+\frac{U}{\eta}\Big) & W' &= \frac{bW}{\eta-U} \\ g' &= \frac{g}{\eta-U}\Big[U' + \Big(d+\frac{U}{\eta}\Big)\Big] & P' &= \frac{V'g}{\eta} - bUg + (\eta-U)gU' \end{aligned} \tag{3.14}$$

Also, applying the similarity transformations on equations (2.3), we obtain the non-dimensional components of the vorticity vector

$$\ell_r = \frac{\zeta_r}{\dot{R}/R} \qquad \ell_\theta = \frac{\zeta_\theta}{\dot{R}/R} \qquad \ell_z = \frac{\zeta_z}{\dot{R}/R}$$

in the flow-field behind the shock as

$$\ell_r = 0 \qquad \ell_\theta = -\frac{1}{2}\frac{bW}{\eta - U} \qquad \ell_z = \frac{V}{2}\Big(\frac{1}{\eta} + \frac{b + U/\eta}{\eta - U}\Big) \tag{3.15}$$

Ordinary differential equations (3.14) with boundary conditions (3.11) can now be numerically integrated to obtain the solution for the flow behind the shock surface.

4. Results and discussion

Similarity considerations lead to the following relations among the constants a, b, d and s

$$a = b \qquad 2b + d = s(1 - b) - 2 \qquad 2d + d > 0 \tag{4.1}$$

Then the following three cases may exist.

(i) The increasing velocity shock $(b > 0)$,

(ii) the constant velocity shock $(b = 0)$, and

(iii) the decreasing velocity shock $(b < 0)$.

Therefore, for the purpose of numerical calculations, we choose the following three sets of values of the constants

(i) $b = 0.5,\ d = -0.5,\ s = 5$;

(ii) $b = 0,\ d = 0.5,\ s = 5/2$;

(iii) $b = -0.5,\ d = 1.5,\ s = 5/3$.

The solutions to differential equations (3.14) with boundary conditions (3.11) depend upon five constant parameters γ, M, A/Q, b and d. Numerical integration of these differential equations is performed to obtain the non-dimensional variables U, V, W, g, P, by using the Runge-Kutta method of the order four, for $\gamma = 1.4$; $M^2 = 5,\ 10$; $A/Q = 0.1$; $b = 0.5,\ 0,\ -0.5$ and $d = -0.5,\ 0.5,\ 1.5$.

The profiles of U, V, W, g and P are shown in Figs. 1 to 5. Also, the non-zero and non-dimensional components ℓ_θ and ℓ_z of the vorticity vector

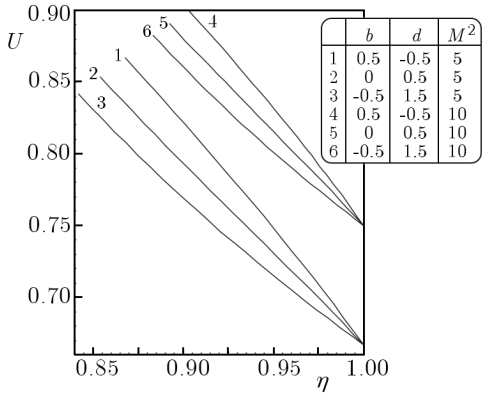

Fig. 1. Variation of the non-dimensional radial velocity U in the flow-field behind the shock front

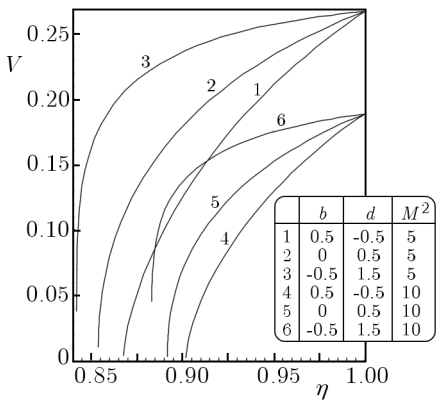

Fig. 2. Variation of the non-dimensional azimuthal velocity V in the flow-field behind the shock front

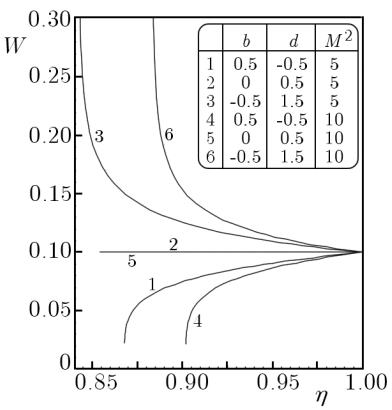

Fig. 3. Variation of the non-dimensional axial velocity W in the flow-field behind the shock front

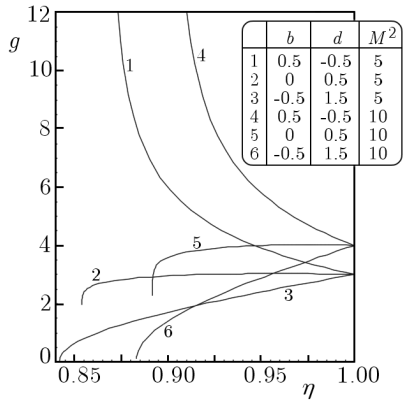

Fig. 4. Variation of the non-dimensional density g in the flow-field behind the shock front

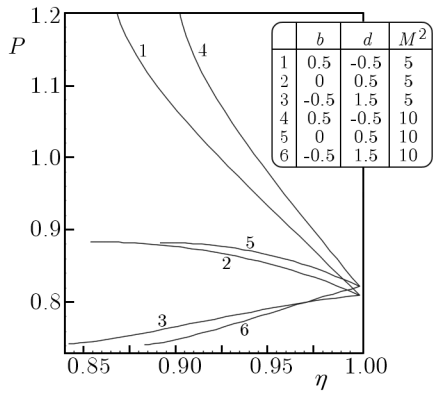

Fig. 5. Variation of the non-dimensional pressure P in the flow-field behind the shock front

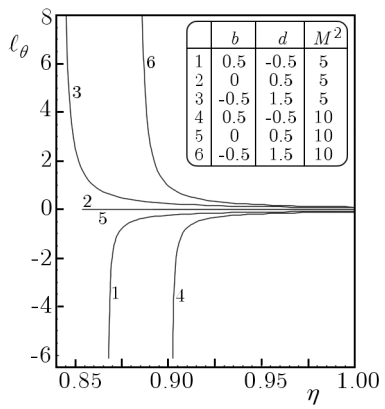

Fig. 6. Variation of the non-dimensional azimuthal component of vorticity ℓ_θ in the flow-field behind the shock front

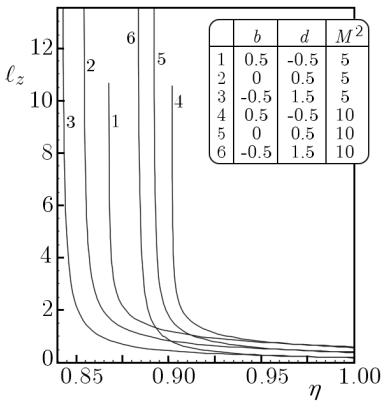

	b	d	M^2
1	0.5	-0.5	5
2	0	0.5	5
3	-0.5	1.5	5
4	0.5	-0.5	10
5	0	0.5	10
6	-0.5	1.5	10

Fig. 7. Variation of the non-dimensional axial component of vorticity ℓ_z in the flow-field behind the shock front

are plotted in Figs. 6 and 7, respectively. Values of η_p (the position of the inner expanding surface) are shown in table 1 for different cases.

Figures 1 and 2 show that the non-dimensional radial velocity U increases from the shock front to the inner expanding surface, whereas the non-dimensional azimuthal velocity V decreases. Figure 3 shows that the non-dimensional axial velocity W increases, remains constant or decreases from the shock front to the inner surface according as $b < 0$, $b = 0$ or $b > 0$, i.e. according as the shock velocity (or initial azimuthal fluid velocity) is decreasing remaining constant or increasing with the shock radius. Figures 4 and 5 show that the non-dimensional density g and pressure P increase or decrease from the shock front to the inner expanding surface according as $b > 0$ or $b < 0$ (i.e. according as the shock velocity is increasing or decreasing with the shock radius). Figure 6 shows that the non-dimensional azimuthal component of vorticity ℓ_θ increases behind the shock front and tends to infinity at the inner surface, remains zero or decreases behind the shock front and tends to negative infinity at the inner surface according as $b < 0$, $b = 0$ or $b > 0$. Figure 7 shows that the non-dimensional axial component of vorticity ℓ_z increases behind the shock front and tends to infinity within a narrow region at the inner surface.

From Table 1 and Figs. 1 to 7, it is found that the effects of the increase in the value of M^2 are

- to increase η_p, i.e. to decrease the distance of the inner expanding surface from the shock front. Physically, it means that the gas behind the shock is compressed, i.e. the shock strength is increased (see Table 1);

- to increase the radial velocity U and to decrease the azimuthal velocity V at any point in the flow-field behind the shock (see Figs. 1 and 2);
- to decrease (or increase) the axial velocity W when the index of variation of the initial azimuthal velocity b has a positive (or negative) value (see Fig. 3); and
- to increase density g and pressure P when b is positive (see Figs. 4 and 5).

Table 1. Position of the inner expanding surface η_p for $\gamma = 1.4$, $A/Q = 0.1$ and various values of M^2, b and d

M^2	b	d	η_p
5	0.5	−0.5	0.8676
	0	0.5	0.8538
	−0.5	1.5	0.8419
10	0.5	−0.5	0.9018
	0	0.5	0.8917
	−0.5	1.5	0.8831

The effects of the increase in the value of the index of variation of the initial azimuthal velocity b of the medium are

- to decrease the distance of the inner expanding surface from the shock front, i.e. to increase the shock strength (see Table 1);
- to increase the radial velocity U and to decrease the azimuthal velocity V and axial velocity W at any point in the flow-field behind the shock (see Figs. 1 to 3);
- to increase the density g and the pressure P at any point in the flow-field behind the shock (see Figs. 4 and 5);
- to decrease ℓ_θ and to increase ℓ_z behind the shock (see Figs. 6 and 7); and
- to increase the shock velocity (see equation (3.16)).

The effects of an increase in the value of the index of variation of the density d are

- to increase the distance of the inner expanding surface from the shock front (see Table 1);
- to decrease the radial velocity U and to increase the azimuthal velocity V and the axial velocity W at any point in the flow-field behind the shock front (see Figs. 1 to 3);

- to decrease the density g and pressure P at any point in the flow-field behind the shock (see Figs. 4 and 5); and
- to increase the vorticity components ℓ_θ and to decrease ℓ_z (see Figs. 6 and 7).

References

1. Chaturani P., 1970, Strong cylindrical shocks in a rotating gas, *Appl. Sci. Res.*, **23**, 1, 197-211
2. Director M.N., Dabora E.K., 1977, An experiment investigation of variable energy blast waves, *Acta. Astronaut.*, **4**, 391-407
3. Freeman R.A., 1968, Variable energy blast waves, *J. Phys.*, **D1**, 1697-1710
4. Lee T.S., Chen T., 1968, Hydromagnetic interplanetary shock waves, *Planet. Space Sci.*, **16**, 1483-1502
5. Levin V.A., Skopina G.A., 2004, Detonation wave propagation in rotational gas flows, *J. Appl. Mech. Tech. Phys.*, **45**, 457-460
6. Nath O., Ojha S.N., Takhar H.S., 1991, A study of stellar point explosion in a self-gravitating radiative magnetohydrodynamic medium, *Astrophys. Space Sci.*, **183**, 135-145
7. Rogers M.H., 1958, Similarity flows behind strong shock waves, *Quart. J. Mech. Appl. Math.*, **11**, 411-422
8. Sakurai A., 1956, Propagation of spherical shock waves in stars, *J. Fluid Mech.*, **1**, 436-453
9. Sedov L.I., 1959, *Similarity and Dimensional Methods in Mechanics*, Academic Press, London
10. Summers D., 1975, An idealised models of a magnetohydrodynamics spherical blast waves applied to a flare produced shock in the solar wind, *Astron. Astrophys.*, **45**, 151-158
11. Vishwakarma J.P., Maurya A.K., Singh K.K., 2007, Self-similar adiabatic flow headed by a magnetogasdynamic cylindrical shock wave in a rotating non-ideal gas, *Geophys. Astrophys. Fluid Dyn.*, **101**, 155-168
12. Vishwakarma J.P., Vishwakarma S., 2007, Magnetogasdynamic cylindrical shock waves in a rotating gas with variable density, *Int. J. Appl. Mech. Engng.*, **12**, 283-297
13. Vishwakarma J.P., Yadav A.K., 2003, Self-similar analytical solutions for blast waves in inhomogeneous atmospheres with frozen-in-magnetic field, *Eur. Phys. J.*, **B 34**, 247-253

14. Zel'dovich Ya.B., Raizer Yu.P., 1967, *Physics of Shock Waves and High Temperature Hydrodynamic Phenomena*, **II**, Academic Press

Rozwiązania automorficzne dla cylindrycznej fali uderzeniowej przy rotacyjnym osiowo-symetrycznym przepływie gazu

Streszczenie

W pracy przedstawiono rozwiązania automorficzne otrzymane dla adiabatycznego przepływu czynnika za cylindryczną fala uderzeniową rozchodzącą się w rotacyjnym, osiowo-symetrycznym opływie gazu doskonałego, którego prędkość początkowa oraz gęstość są funkcjami odległości od osi symetrii. W stanie początkowym, analizowany czynnik posiada oprócz zmiennej składowej osiowej prędkości dodatkowo zmienną składową azymutalną. Założono, że prędkości początkowe i gęstość opisują funkcje potęgowe. Rozkłady prędkości płynu, gęstość, ciśnienie oraz składowe wirowości otrzymano w polu przepływu za frontem fali uderzeniowej. Zbadano także wpływ prędkości początkowych oraz gęstości na zmiany wartości liczby Macha.

Manuscript received April 8, 2011; accepted for print October 26, 2011